Preparation of N-doped hydrogen-free diamondlike carbon and its application to field emitters

Jong Hyun Moon, Suk Jae Chung, Eun Jung Han, and Jin Jang[a)]
Department of Physics, Kyung Hee University, Dongdaemoon-ku, Seoul 130-701, Korea

Jae Hoon Jung, Byeong Kwon Ju, and Myung Hwan Oh
Electronic Materials and Devices Research Center, Korea Institute of Science and Technology, Seoul 130-650, Korea

(Received 26 February 1998; accepted 23 October 1998)

We have studied the electrical, optical and field emission properties of nitrogen gas-phase doped hydrogen-free diamondlike carbon (DLC) films. The N-doped hydrogen-free DLC films were deposited by an alternating layer deposition technique using plasma enhanced chemical vapor deposition, in which deposition of a thin layer of gas-phase doped DLC and CF_4 plasma exposure on its surface were carried out alternately. The optical band gap of the DLC films decreases from 1.8 to 1.55 eV with an increase of the $[N_2]/[CH_4]$ ratio from 0% to 24% because of an increase of the graphite phase (π state). The emission current density and onset field are strongly related to the gas-phase doping concentration in the DLC films. The optimum $[N_2]/[CH_4]$ flow rate ratio for efficient electron emission was found to be 9%. The onset field and the effective barrier energy at 9% are 7.2 V/μm and 0.02 eV, respectively. The material appears to be modified into a carbon-nitrogen alloy when it exceeds 9%. We have also studied the enhanced field emission characteristics of nitrogen gas-phase doped hydrogen-free DLC films on Mo tip field emitter arrays. The maximum emission current for each pixel increased from 160 μA to 1.52 mA with the addition of a 200 Å thick N doped hydrogen-free DLC coating on the Mo tips. © *1999 American Vacuum Society.* [S0734-211X(99)01601-7]

I. INTRODUCTION

Field emitter arrays (FEAs) are becoming increasingly important as micron size electron sources for a number of advanced and new generation devices such as field emission displays (FEDs), ultrahigh-frequency devices.[1,2] Highly efficient and highly reliable FEAs require a sharp emitter tip, reduced emitter to gate distance, lower work function emitter materials and improved uniformity and reproducibility.[3,4]

The low voltage operation of FEAs allows the FEAs to operate continuously with very stable emission properties and long life, at pressures higher than those necessary for conventional field emitters, and without resorting to the stratagems of intermittent or continuous heating. Diamond films possessing negative electron affinity (NEA)[5] have great potential for application as electron emitters in vacuum microelectronics such as FEAs and have been the focus of extensive study. The interest in diamondlike carbon (DLC) as an emission material originates from its unique emission properties and because of its low work function and its stable operation.

For FED applications, the work function of the emitter is important in order to have low voltage driving. C-Si and metals have high work functions (~4.5 eV), requiring the formation of sharp tips, and the surface of the tips is unstable during operation because of aging by oxidation. However, the work function of DLC is lower than that of *c*-Si or metals. Furthermore, the work function can be controlled by impurity doping[6] and there is no aging effect for DLC film because of its chemical inertness.

Therefore, cold cathode electron emitters obtained by depositing diamond films on Si FEAs,[7] Mo FEAs,[8] or W FEAs (Ref. 9) have been widely studied. The field strength required for electron field emission has been reduced to less than 3×10^4 V/cm, which is substantially lower than the field strength used in conventional metal FEAs, which are typically higher than 1×10^6 V/cm.[10] Chuang *et al.*[10] have already reported DLC coated Mo FEAs using a laser ablation process. But the DLC layer suffers from emission instability because the surface of the DLC is deteriorated by local heating during operation.

In our previous work, an alternating layer deposition method, i.e., the deposition of a thin DLC layer and subsequent exposure of its surface to CF_4 plasma, was applied to deposit hydrogen-free DLC film.[11]

In this study, we report on the electrical, optical and electron emission properties of gas-phase nitrogen-doped, hydrogen-free DLC films with various $[N_2]/CH_4]$ flow rate ratios. Also, the fabrication of a N-doped hydrogen-free DLC film coating onto a Mo FEA and its enhancement of the field emission characteristics will be discussed.

II. EXPERIMENT

For the deposition of nitrogen-doped hydrogen-free DLC, we have used a conventional plasma enhanced chemical vapor deposition (PECVD) system, in which rf power was applied to the substrate holder. $N_2/CH_4/H_2/He$ and CF_4/He gases were introduced for deposition of the DLC layer and for the surface treatment, respectively.

Table I depicts the alternating layer deposition conditions for the nitrogen-doped DLC films. The flow rates of He, H_2,

[a)]Electronic mail: jjang@nms.kyunghee.ac.kr

TABLE I. Alternating layer deposition conditions for the N-doped DLC films.

Condition	Deposition	CF_4 plasma exposure
Radio frequency power (W)	100	100
Pressure (mbar)	0.4	0.45
Flow rate (sccm)		
He	20	20
H_2	6	0
N_2	0.09–1.5	0
CH_4	3	0
CF_4	0	20
Substrate temperature (K)	300	300
Time (s)	95	140

and CH_4 were fixed at 20, 6 and 3 sccm, respectively, and the $[N_2]/[CH_4]$ flow rate ratio was changed from 3% to 50% by varying the N_2 flow rate. The CF_4 flow rate and CF_4 plasma exposure time were fixed at 20 sccm and 140 s, respectively, for the plasma treatment. Details of the alternating layer deposition method are described in the literature.[11,12] The self-bias voltage measured was found to be -120 V at a fixed rf power of 100 W.

The absorption coefficients for the CH_n ($n=1$, 2, 3) stretching modes were measured by a Fourier transform infrared spectrophotometer, and the hydrogen content was determined using the integrated absorption coefficients of CH_n modes.[13] It was found that the hydrogen content decreases with increasing CF_4 plasma exposure time and is zero at an exposure time of 140 s.[11,12] Also, it was confirmed that the hydrogen content is less than 1 at. % at the CF_4 plasma exposure of 140 s by secondary ion mass spectroscopy (SIMS) analysis.

We fabricated the Mo FEAs by the process used for conventional Spindt-type FEAs.[14] After that, we deposited a 200 Å thick N-doped hydrogen-free DLC film onto the Mo FEAs by repeating five cycles of deposition and CF_4 plasma exposure.

The field emission cathode consists basically of a conductor/insulator/conductor sandwich. The top conductor or gate film has a 1.5 μm diam hole in it, through which a cavity into the insulator can be etched. This cavity undercuts the gate and uncovers the substrate conductor.

A metal cone whose base is attached to the substrate and whose tip is close to the plane of the gate film is then formed in the cavity.[15]

A heavily doped silicon wafer, n^{++}-Si, is preferred as the substrate, because thermal silicon dioxide (SiO_2) can be grown on its surface to a thickness of 1.2 μm with excellent adherence, no porosity, and high-field breakdown strength. A film of chromium (Cr), about 0.4 μm thick, is deposited by rf magnetron sputtering onto the silicon dioxide to provide a gate electrode.

Cathodes with 900 emitting cones per one pixel have been grown. The 900 cone array was arranged in a 30×30 matrix with 10 μm spacing, and the total cathode area covers a square that is 300 μm on each side.

The interband optical absorption coefficients were measured using a Perkin-Elmer ultraviolet (UV) visible (vis) infrared (IR) spectrophotometer and the optical band gap was obtained using Tauc's plot. The current-electric field (*I-E*) characteristics of the film were measured between two parallel plates in vacuum of 10^{-7} Torr to characterize the electron emission properties.

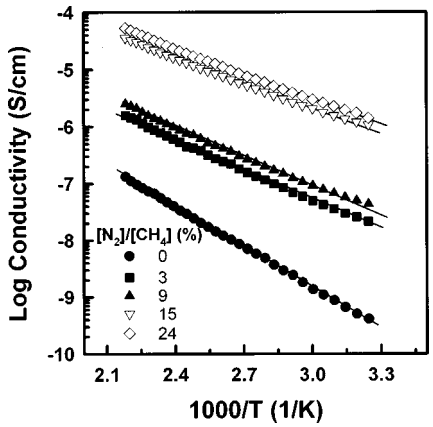

FIG. 1. N-doped hydrogen-free DLC film, showing the temperature dependence on the electrical conductivities with various nitrogen gas flow ratios.

The electron emission characteristics of the FEAs were measured using a triode geometry. An anode plate was placed 300 μm above the gate and was biased to 0–700 V. Both the anode-to-cathode and the gate-to-cathode currents were measured as a function of bias voltage using a Keithley SMU 237 under ultrahigh vacuum of 1×10^{-8} Torr.

During the measurement, the device was in a common emitter configuration with the emitter grounded and both the anode and gate being at positive potentials.

III. RESULTS AND DISCUSSION

A. Electrical and optical properties of N-doped hydrogen-free DLC films

Figure 1 shows temperature dependent conductivity of the N-doped hydrogen-free DLC films deposited with various nitrogen gases. The conductivity increases from $4.1\times10^{-10}$to 1.4×10^{-6} S/cm when the $[N_2]/[CH_4]$ ratio changes from 0% to 24%, because the Fermi level is shifted toward the conduction band by *n*-type doping. When the $[N_2]/[CH_4]$ ratio is above 15%, the conductivity steadily increases. The nitrogen appears to be a shallow donor in DLC and the gradual shift of the Fermi level toward the conduction band by the nitrogen atom is confirmed. The conductivity increases and thus the activation energy decreases with the increasing $[N_2]/[CH_4]$ ratio when the $[N_2]/[CH_4]$ ratio is less than 15%, but after that the conductivity increases steadily due to the continuous shift of the Fermi level toward the conduction band, caused by nitrogen atoms accumulated in the DLC films.

Figure 2 shows Tauc's plots of the N-doped DLC films with various $[N_2]/[CH_4]$ ratios. The *B*, obtained from the slope of Tauc's plot: $(\alpha h\nu)^{1/2}=B(h\nu-E_g)$, where α is the absorption coefficient, E_g is the optical band gap and $h\nu$ is

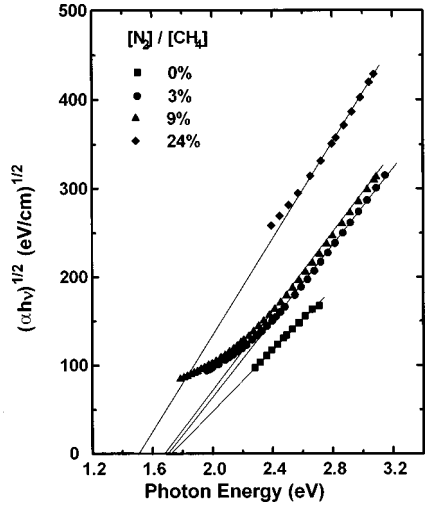

FIG. 2. Tauc's plots of N-doped hydrogen-free DLC films with various nitrogen gas flow ratios.

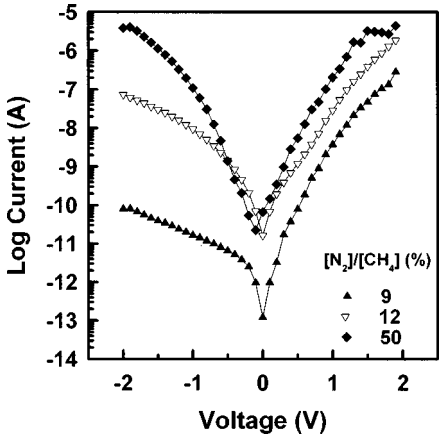

FIG. 4. Current-voltage characteristics for Al/N-doped hydrogen-free DLC/p^+-Si devices with various nitrogen gas flow ratios.

the photon energy, increases with increasing nitrogen doping. The increase in the slope which is related to incorporation of N atoms, causes the conversion of sp^3 C to sp^2 C.[16] Note that the conversion of sp^3 to sp^2 reduces the band gap of the DLC film.[16]

Figure 3 shows the optical band gap (E_g^{opt}) obtained from Tauc's plot for the DLC films. It decreases from 1.8 to 1.55 eV with an increase of the $[N_2]/[CH_4]$ ratio from 0% to 24%. The decrease in the optical band gap appears to be due to the increase of the graphite phase in the DLC as a result of nitrogen incorporation, as is also the case for tetrahedral amorphous carbon (ta-C).[4]

We have also studied the current-voltage characteristics of an Al/DLC/p^+-Si device. The N-doped hydrogen-free DLC films were deposited on a low resistivity p^+-Si (100) wafer and then the aluminum dots were thermally evaporated before the I–V characteristics were measured.

Figure 4 shows the I–V characteristics for the Al/N-doped hydrogen-free DLC film/p^+-Si device with various nitrogen flow rates. The n-type conduction appears because the Fermi level for the DLC film is shifted toward the conduction band and the carrier concentration of the conduction band of the DLC film increases by the substitutional doping of nitrogen atoms.

Both the shift of the Fermi level and the increase of the carrier concentration for the DLC cause the increase of electron emission current for the N-doped hydrogen-free DLC film. The shift of the Fermi level causes a decrease in the work function, which was deduced from the decrease in the slope of the Fowler-Nordheim (FN) plot resulting from the DLC coating. We can see that the decrease of the work function causes an increase of emission current and a decrease of turn-on voltage.

The diode with 9% N doping shows the lowest reverse current and the lowest diode quality factor because of the lower density of states in the gap of the DLC. There is no direct relationship between the diode characteristics and the emission properties of the DLC, but the 9% doped DLC shows the best diode and field emitter characteristics.

In the region of the $[N_2]/[CH_4]$ ratio above 12%, the defect states seem to be generated in the DLC film and then the film structure changes into another structure, for example, a C-N alloy. As a result, the current-voltage characteristics for 50% gas-phase N-doped DLC film show a symmetric behavior in Fig. 4 because of the high density of state in the gap of the DLC.

The depth profiles of nitrogen and carbon atoms in the N-doped hydrogen-free DLC film deposited with a $[N_2]/[CH_4]$ ratio of 9% were measured by x-ray photoelectron spectroscopy (XPS). Except for the surface region (20 nm from the surface) of the DLC film, it shows a uniform N concentration and the incorporated nitrogen concentration in the DLC film is 1.99 at. %.

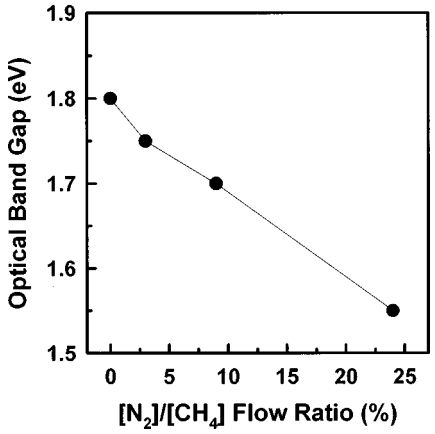

FIG. 3. Optical band gap of N-doped hydrogen-free DLC films with various nitrogen gas flow ratios.

B. Field emission properties of DLC and Mo tip FEAs

When considering the possible use of ta-C and DLC as cold cathode materials, control of the Fermi energy through

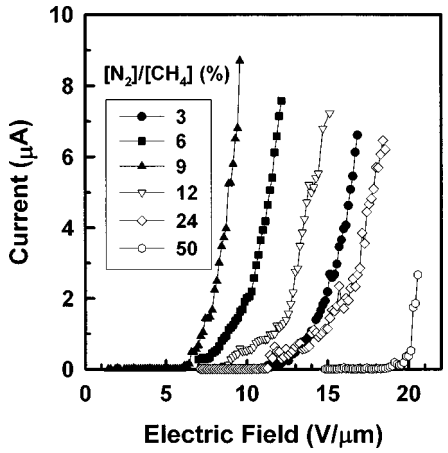

FIG. 5. Current-electric field characteristics for N-doped hydrogen-free DLC films with various nitrogen gas flow ratios.

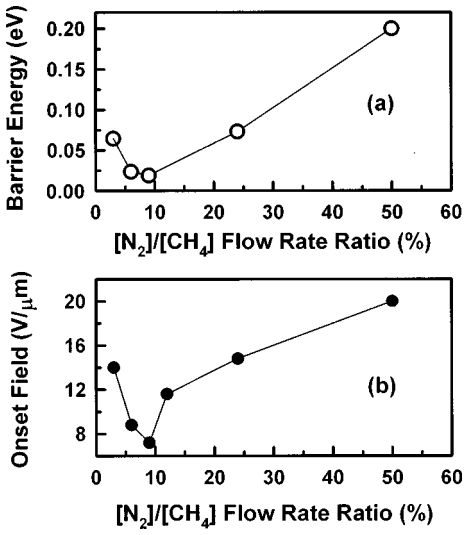

FIG. 7. (a) Effective barrier energy and (b) onset field for N-doped hydrogen-free DLC films with various nitrogen gas flow ratios.

the band gap by doping should be done to reduce its work function. The work function is related to the turn-on field for electron emission.

The successful *n*-type doping of *ta*-C by nitrogen incorporation is possible without changing its tetrahedral structure.[17] Nitrogen, a deep donor in diamond, occupies a substitutional site distorted along the (111) direction.[18]

Figure 5 shows the *I–E* characteristics of the nitrogen-doped DLC films. The electron emission current increases at first with the $[N_2]/[CH_4]$ ratio up to 9% and then it decreases with a further increase of the $[N_2]/[CH_4]$ ratio. The optimum $[N_2]/[CH_4]$ ratio appears to be 9%. The onset field decreases at first with the $[N_2]/[CH_4]$ ratio up to 9% and then it increases with a further increase of the $[N_2]/[CH_4]$ ratio. At a 9% $[N_2]/[CH_4]$ ratio, it shows a minimum value of the onset field. Also, electron emission current at the 10 V/μm has a maximum value at a 9% $[N_2]/[CH_4]$ ratio because of the shift of the Fermi level and the subsequent increase of the carrier density.

The low current tails in the 6% and 12% data can be seen in Fig. 5 and these tails may be related with the film structure and chemical composition, but more work is needed to clarify their origin.

Figure 6 shows a FN plot of the electron emission currents for the N-doped DLC films. The slope of the FN plot is related to the effective work function of the film. It decreases to 0.02 eV with an increase in the $[N_2]/[CH_4]$ ratio until 9% and then increases. The effective barrier energy for the DLC deposited with a 50% $[N_2]/[CH_4]$ ratio is 0.2 eV.

Figures 7(a) and 7(b) show the effective barrier energy and the onset field of the electron emission current, respectively, for the N-doped DLC films. The onset field and effective barrier energy are 7.2 V/μm and 0.02 eV, respectively, at the optimum condition of a 9% $[N_2]/[CH_4]$ ratio.

Figure 8 shows a comparison of the emission current-voltage characteristics between N-doped DLC coated Mo FEAs and noncoated Mo FEAs composed of 900 emitters for one pixel. The turn-on voltage decreases from 60 to 27 V due to the N-doped DLC coating. In addition to the decrease

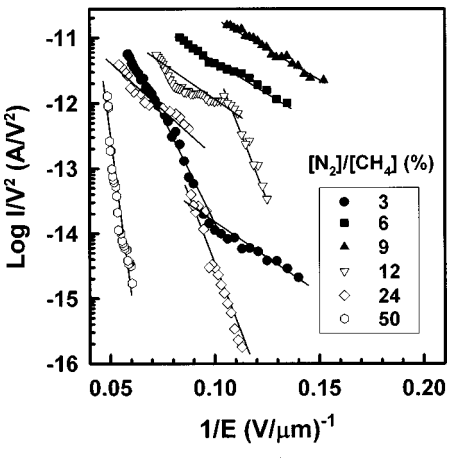

FIG. 6. Fowler-Nordheim plots for N-doped hydrogen-free DLC films with various nitrogen gas flow ratios.

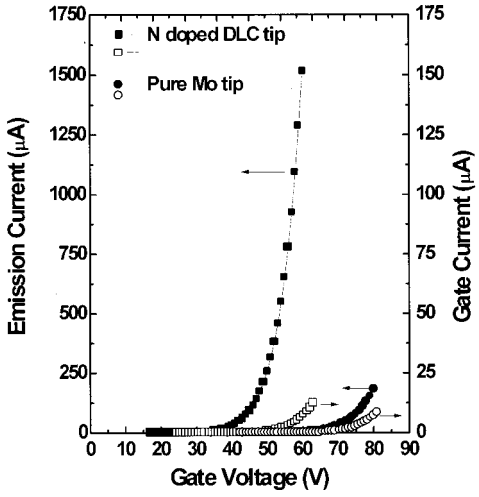

FIG. 8. Emission current-voltage characteristics for N-doped hydrogen-free DLC coated Mo FEAs and noncoated Mo FEAs.

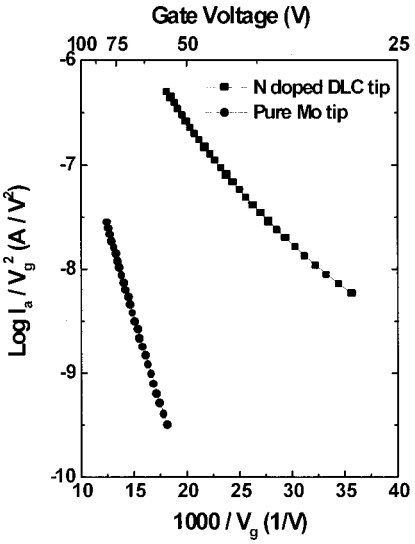

FIG. 9. Fowler-Nordheim plots for N-doped hydrogen-free DLC coated Mo FEAs and Mo FEAs without the DLC film.

in turn-on voltage, the anode current is also increased from 160 μA to 1.52 mA. This indicates that the operating voltage of the FED can be remarkably decreased by adding a N-doped DLC layer on Mo FEAs. The increase of emission current is related to the shift of the Fermi level and the subsequent increase of carrier density in the DLC film. The current between the gate and emitters is less than 0.9% of the current between the anode and emitters for the N-doped DLC coated Mo FEAs, but less than 6.25% for the Mo FEAs.

Figure 9 shows a comparison of FN plots between N-doped DLC coated Mo FEAs and noncoated Mo FEAs. The field enhancement factor (β) for the emitter was first obtained by comparing the work function (ϕ) value calculated from the slope of the FN plots of the Mo FEAs with the work function reported for Mo metal (4.5 eV). The effective work function ϕ values calculated for the Mo FEAs and for the N-doped hydrogen-free DLC coated FEAs are 4.5 and 1.9 eV, respectively, both of which are much less than that of the Mo work function, and the effective work function once again seems to be lowered by the DLC coating. This indicates that the operating voltage can be remarkably decreased by adding a N-doped DLC layer on Mo FEAs.

The *n*-type doping in DLC film has been thought to be very difficult due to the high density of states in the gap near the Fermi level and the autocompensation effect, in which doping is accompanied by an increased defect density.[19] Auto-compensation is the reason why the doping efficiency of DLC film is much lower than that of hydrogenated amorphous silicon (*a*-Si:H). In DLC, relatively low E_d (defect creation energy) of π-like defects (those lower than 0.4 eV) result in greater compensation and a much lower doping efficiency.

IV. CONCLUSION

The electrical, optical and electron emission properties of gas-phase nitrogen-doped DLC films with various $[N_2]/[CH_4]$ flow rate ratios have been studied. The optical band gap of DLC films decreases from 1.8 to 1.55 eV with an increase in the $[N_2]/[CH_4]$ ratio from 0% to 24% because of the increase of the graphite phase (π states).

The emission current density and onset field are strongly related to the gas-phase doping concentration in the DLC films. The optimum $[N_2]/[CH_4]$ flow rate ratio for efficient electron emission was found to be 9%. The onset field and effective barrier energy for electron emission at 9% are 7.2 V/μm and 0.02 eV, respectively. The material appears to be modified to a carbon-nitrogen alloy when it exceeds 9%. Also, enhancement of the field emission characteristics by the nitrogen gas-phase doped hydrogen-free DLC coating on Mo FEAs was found. The maximum emission current for each pixel was increased from 160 μA to 1.52 mA by a 200 Å thick N-doped hydrogen-free DLC films coating onto the Mo tips.

ACKNOWLEDGMENTS

This work was supported by the Korea Science and Engineering Foundation (95-0300-15-01-3) and by the Ministry of Education through the Basic Science Research Institute Program (BSRI-97-2443).

[1]C. A. Sindt, I. Bodie, L. Humphrey, and E. R. Westerberg, J. Appl. Phys. **47**, 5248 (1976).
[2]P. Vaudaine and R. Meyer, Tech. Dig. Int. Electron Devices Meet. 197 (1991).
[3]H. H. Busta, J. E. Pogemiller, and B. J. Zimmerman, J. Vac. Sci. Technol. B **12**, 689 (1994).
[4]M. Nakamoto, T. Hasegawa, T. Ono, T. Skai, and N. Sakuma, Tech. Dig. Int. Electron Devices Meet. 297 (1996).
[5]F. J. Himpsel, J. A. Knapp, and J. A. Van Vechten, Phys. Rev. B **20**, 624 (1979).
[6]J. D. Lamb and J. A. Woollam, J. Appl. Phys. **57**, 5420 (1985).
[7]J. Liu, V. V. Zhirnov, A. F. Myer, G. J. Wojak, W. B. Choi, J. J. Hren, S. D. Wolter, T. McClure, B. R. Stoner, and J. T. Glass, J. Vac. Sci. Technol. B **13**, 422 (1995).
[8]W. B. Choi, J. Liu, M. T. McClure, A. F. Myers, J. J. Cuomo, and J. J. Hren, Proceedings of the 8th International Vacuum Microelectronics Conference, Portland, 1995, p. 315.
[9]N. Liu, Z. Ma, X. Chu, T. Hu, Z. Xue, X. Jiang, and S. Pang, J. Vac. Sci. Technol. B **12**, 1712 (1994).
[10]F. Y. Chang, C. Y. Sun, H. F. Cheng, C. M. Huang, and I. N. Lin, Appl. Phys. Lett. **68**, 1666 (1996).
[11]K. C. Park, J. H. Moon, and J. Jang, Appl. Phys. Lett. **68**, 3594 (1996).
[12]K. C. Park, J. H. Moon, C. J. Chung, M. H. Oh, W. I. Milne, and J. Jang, Appl. Phys. Lett. **70**, 1381 (1997).
[13]K. Nakazawa, S. Ueda, M. Kumeda, A. Morimoto, and T. Shimizu, Jpn. J. Appl. Phys., Part 2 **21**, L617 (1992).
[14]J. H. Jung, B. K. Ju, Y. H. Lee, M. H. Oh, and J. Jang, Tech. Dig. Int. Electron Devices Meet. 293 (1996).
[15]C. A. Spindt, K. R. Shoulders, and L. N. Heynick, U.S. Patent No. 3,755,704 (1973).
[16]V. S. Veerasamy, J. Yuan, G. A. J. Amaratunga, W. I. Milne, K. W. R. Gilkes, M. Weiler, and L. M. Brown, Phys. Rev. B **48**, 17954 (1993).
[17]V. S. Veerasamy, G. A. J. Amaratunga, C. A. Davis, A. E. Timbs, W. I. Milne, and D. R. Mackenzie, J. Phys.: Condens. Matter **5**, 169 (1993).
[18]S. A. Kajihara, A. Antonelli, J. Bernholc, and R. Car, Phys. Rev. Lett. **66**, 2010 (1991).
[19]J. Robertson, Phys. Rev. B **33**, 4399 (1986).